



Functional and molecular characterisation of EO771.LMB tumours, a new C57BL/6-mouse-derived model of spontaneously metastatic mammary cancer.

AUTHOR(S)

Cameron N. Johnstone, Yvonne Smith, Yuan Cao, Allan D. Burrows, Ryan SN Cross, Xiawei Ling, Richard P. Redvers, Judy P. Doherty, Bedrich L. Eckhardt, Anthony L. Natoli, Christina M. Restall, Erin Lucas, Helen B. Pearson, Siddhartha Deb, Kara L. Britt, Alexandra Rizzitelli, Jason Li, Judith Harmey, Normand Pouliot, Robin L. Anderson

CITATION

Johnstone, Cameron N.; Smith, Yvonne; Cao, Yuan; Burrows, Allan D.; Cross, Ryan SN; Ling, Xiawei; et al. (2015): Functional and molecular characterisation of EO771.LMB tumours, a new C57BL/6-mouse-derived model of spontaneously metastatic mammary cancer.. Royal College of Surgeons in Ireland. Journal contribution. <https://hdl.handle.net/10779/rcsi.10783490.v2>

HANDLE

[10779/rcsi.10783490.v2](https://hdl.handle.net/10779/rcsi.10783490.v2)

LICENCE

CC BY-NC-SA 4.0

This work is made available under the above open licence by RCSI and has been printed from <https://repository.rcsi.com>. For more information please contact repository@rcsi.com

URL

https://repository.rcsi.com/articles/journal_contribution/Functional_and_molecular_characterisation_of_EO771_LMB_tumours_a_new_C57BL_6-mouse-derived_model_of_spontaneously_metastatic_mammary_cancer_/10783490/2

Supplementary Figure Legends

Figure S1: Histological classification of murine mammary tumours. (A) EO771 and EO771.LMB primary tumours were sectioned (3 μ m), stained with haematoxylin and eosin (H&E), and compared to 67NR and 4T1.2 primary tumours. H&E stained sections from at least two primary tumours of each tumour type were assessed by a qualified breast pathologist in accordance with the Bloom Richardson Ellis classification system (Elston and Ellis, 2002). Circles indicate highly pleomorphic nuclei. (B) An overall grade was calculated dependent on tubular differentiation/formation (score 1: >75% of tumor area forming glandular/tubular structures, score 2: 10% to 75% and score 3: <10%), nuclear pleomorphism (score 1: nuclei with little increase in size in comparison with normal breast epithelium with minimal variation in size, score 2: larger nuclei with moderate variability and visible nucleoli and score 3: marked nuclear variation with prominent nucleoli) and tumour mitotic count determined by numbers of mitosis seen in 10 consecutive high power fields (score 1: <9 mitosis per 10 HPF, score 2: 9-17 mitosis per 10 HPF, score 3: 18 or more mitosis per 10 HPF). Adding the scores for each parameter determined tumour grade as follows: grade 1 - scores 3,4 and 5, grade 2 - scores 6 and 7, grade 3 - scores 8 and 9.

Black scale bars represent 100 μ m. White circles denote highly pleomorphic nuclei.

Figure S2: Whole lungs were dissected from mice inoculated with the indicated tumour lines and stained with India ink. The number of metastatic nodules on the surface of each lung was counted. $P = 0.20$ (Mann-Whitney test).

Figure S3: Experimental lung metastasis assay. EO771 or EO771.LMB cells were inoculated into C57Bl/6 mice via the tail vein. 19 days later, the metastatic burden in the lung was analyzed by TaqMan qPCR. $P = 0.51$ (Student's t test).

Figure S4: The cell lines indicated were cultured on plastic or monomeric type I bovine collagen (PureCol, Advanced Biomatrix, Carlsbad, CA) for at least 2 days. Images (x100 magnification) were generated using a Leica DM IRB inverted microscope (Leica Microsystems, North Ryde, NSW, Australia).

Figure S5: Anchorage independent growth in soft agar. Colonies in soft agar were stained with calcein^{AM} and fluorescent images generated. The number of colonies $> 50 \mu\text{m}$ in size were counted in three fields per well and averaged. The graph depicts the average number of colonies per field across three wells \pm SD. Differences in colony forming ability between EO771 and EO771.LMB were not significant (Student's t test).

Figure S6: Mammosphere forming capacity of EO771 and EO771.LMB cells in vitro. Representative images from primary (A) and secondary (B) mammosphere cultures from EO771 and EO771.LMB (LMB) are shown. Scale bar = 200 μm . (C) Mammospheres from primary or secondary cultures were enumerated after 10 or 7 days of growth, respectively, and expressed as the mean number of mammospheres per 10 fields \pm SEM. No significant differences in mammosphere number was found between EO771 and EO771.LMB in either primary or secondary cultures. (D) The graph depicts mean mammosphere area in $\mu\text{m}^2 \pm$ SEM for primary and secondary cultures after 10 or 7 days of growth, respectively. The number of individual

mammospheres measured in each condition is indicated above the bars. n/s, not significant.

Figure S7: Adhesion of 67NR and 4T1.2 tumour cells to different substrates after 30min. Adhesion is presented as the percentage of total cell input (mean of triplicate wells \pm SD of one of three representative experiments). *, $P < 0.05$.

Figure S8: ER α -positive human breast cancer cells (MCF7, top panels) or ER α -negative human breast cancer cells (MDA-MB-231, bottom panels) were grown as xenografts in the mammary glands of immunodeficient mice. Tumour sections were stained with anti-human ER α antibody (left panels) or an isotype control antibody (right panels). Scale bars represent 100 μ m.

Figure S9: Distribution of eight gene expression signatures across 67NR, 4T1.2, EO771, and EO771.LMB primary tumours displayed as heat maps. Triplicate tumour specimens are indicated along the X axes and individual genes are shown on the Y axes. Gene expression signatures were obtained from the following references or from

| the | Molecular | Signatures | Database |
|---|-----------|------------|----------|
| (http://www.broadinstitute.org/gsea/msigdb/index.jsp) | | | |
| (A) Basal epithelial (54 genes) | | | |
| (Huper and Marks, 2007), (B) luminal epithelial (59 genes) | | | |
| (Huper and Marks, 2007), (C) proliferation (97 genes) | | | |
| (Ghazoui et al., 2011), (D) hypoxia-regulated (75 genes) | | | |
| (Ghazoui et al., 2011), (E) interferon-regulated (27 genes) | | | |
| (Einav et al., 2005), (F) cancer invasion (64 genes) | | | |
| (Kim et al., 2010), (G) EMT (91 genes) | | | |
| (Taube et al., 2010), (H) breast cancer stem cells (94 genes) | | | |
| (Creighton et al., 2009). | | | |

Figure S10: Venn diagrams were generated from Affymetrix array data showing genes significantly (unadjusted $P < 0.05$) upregulated (**A**), or downregulated (**B**) in 4T1.2 v 67NR (red) and EO771.LMB v EO771 (green). P values were determined by one-way ANOVA using Partek Genomics Suite v6.6. 205 genes were commonly upregulated and 220 genes commonly downregulated in both isogenic tumour comparisons.

Figure S11: qRT-PCR data showing mRNA expression levels of MMP-3 (A), Pthrp (B), S100a8 (C), S100a9 (D), Cd36 (E) and GlyCAM1 (F) in whole 67NR, 4T1.2, EO771 and EO771.LMB (LMB) primary tumours. Three different primary tumours were analysed in duplicate for each tumour model. Thus, each data point represents the mean \pm SD of 6 qRT-PCR reactions across 3 tumours. Expression levels in normal adult mouse mammary gland (MG) were included for each gene for comparison and set to 1. Values on the Y axis represent mRNA expression levels of the gene of interest normalised to Rps27a. *, $P = 0.05$; **, $P < 0.01$; ***, $P < 0.005$; n/s, not significant.

Figure S12: qRT-PCR data showing mRNA expression levels of MMP-3 (A), Pthrp (B), S100a8 (C), S100a9 (D), Cd36 (E) and GlyCAM1 (F) in 67NR, 4T1.2, EO771 and EO771.LMB (LMB) cell cultures. Each data point represents the mean \pm SD of triplicate qRT-PCR reactions. Expression levels in the immortalised mouse mammary epithelial cell line NMuMG were included for comparison and set to 1. Values on the Y axis represent mRNA expression levels of the gene of interest normalised to Rps27a. *, $P < 0.05$; **, $P < 0.01$; n/s, not significant; n/e, not expressed.

Figure S13: Kaplan-Meier survival curves (disease-free survival) for selected genes in primary human breast cancer samples. The BreastMark database (<http://glados.ucd.ie/BreastMark/index.html>) was analyzed for the individual genes indicated above the curves for all patients (all, upper row) or in basal-like tumours only (basal, lower row). Gene expression was measured in primary tumours using Affymetrix microarrays (Madden et al., 2013) A median split was used to allocate 50% of tumours to the "high expression" category (blue curve) and 50% to the "low expression" category (red curve). Patient clinical follow-up was for at least 200 months (X axes). A logrank P value ≤ 0.05 was considered statistically significant. s, significant, n/s, not significant.

Supplementary Table 1: Eight different expression signatures were analysed across four murine mammary cancer models (67NR, 4T1.2, EO771, EO771.LMB) using the R program. The Table depicts the number of genes and percentage of genes (in parentheses) within each signature that were significantly ($P < 0.05$) upregulated (UP), or significantly ($P < 0.05$) downregulated (DOWN) in 67NR, 4T1.2, EO771, or EO771.LMB tumours relative to the mean expression level of each gene across all 15 tumours analyzed (see Materials and Methods). The number and percentage of genes within each signature that were not significantly deregulated is also indicated. Yellow highlighting indicates tumour types where $\geq 25\%$ of the genes within the signature were significantly upregulated, and were thereby considered enriched for the signature. The enriched gene expression signatures are summarised at the bottom of the Table.

Supplementary Table 2: Genes significantly **downregulated** (unadjusted $P < 0.05$, n=220) in both 4T1.2 v 67NR and EO771.LMB v EO771 comparisons. P values were determined by one-way ANOVA using Partek Genomics Suite v6.6.

Supplementary Table 3: Genes significantly **upregulated** (unadjusted $P < 0.05$, n=205) in both 4T1.2 v 67NR and EO771.LMB v EO771 comparisons. P values were determined by one-way ANOVA using Partek Genomics Suite v6.6.

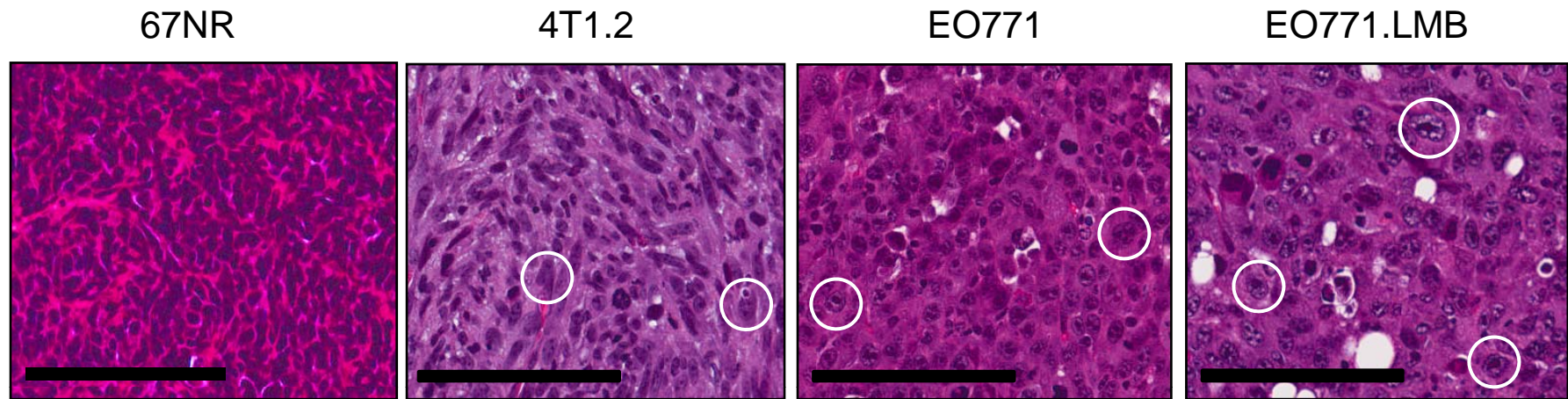
Supplementary Table 4: Sequences of oligonucleotide primers used for SYBR-green qRT-PCR.

Supplementary References

- Creighton, C. J., Li, X., Landis, M., Dixon, J. M., Neumeister, V. M., Sjolund, A., Rimm, D. L., Wong, H., Rodriguez, A., Herschkowitz, J. I. et al.** (2009). Residual breast cancers after conventional therapy display mesenchymal as well as tumor-initiating features. *Proc. Natl. Acad. Sci. U. S. A.* **106**, 13820-5.
- Einav, U., Tabach, Y., Getz, G., Yitzhaky, A., Ozbek, U., Amariglio, N., Izraeli, S., Rechavi, G. and Domany, E.** (2005). Gene expression analysis reveals a strong signature of an interferon-induced pathway in childhood lymphoblastic leukemia as well as in breast and ovarian cancer. *Oncogene* **24**, 6367-75.
- Elston, C. W. and Ellis, I. O.** (2002). Pathological prognostic factors in breast cancer. I. The value of histological grade in breast cancer: experience from a large study with long-term follow-up. *Histopathology* **41**, 154-61.
- Ghazoui, Z., Buffa, F. M., Dunbier, A. K., Anderson, H., Dexter, T., Detre, S., Salter, J., Smith, I. E., Harris, A. L. and Dowsett, M.** (2011). Close and stable relationship between proliferation and a hypoxia metagene in aromatase inhibitor-treated ER-positive breast cancer. *Clin. Cancer Res.* **17**, 3005-12.
- Huper, G. and Marks, J. R.** (2007). Isogenic normal basal and luminal mammary epithelial isolated by a novel method show a differential response to ionizing radiation. *Cancer Res.* **67**, 2990-3001.
- Kim, H., Watkinson, J., Varadan, V. and Anastassiou, D.** (2010). Multi-cancer computational analysis reveals invasion-associated variant of desmoplastic reaction involving INHBA, THBS2 and COL11A1. *BMC Med. Genomics* **3**, 51.
- Madden, S. F., Clarke, C., Gaule, P., Aherne, S. T., O'Donovan, N., Clynes, M., Crown, J. and Gallagher, W. M.** (2013). BreastMark: an integrated approach to mining publicly available transcriptomic datasets relating to breast cancer outcome. *Breast Cancer Res.* **15**, R52.

Taube, J. H., Herschkowitz, J. I., Komurov, K., Zhou, A. Y., Gupta, S., Yang, J., Hartwell, K., Onder, T. T., Gupta, P. B., Evans, K. W. et al. (2010). Core epithelial-to-mesenchymal transition interactome gene-expression signature is associated with claudin-low and metaplastic breast cancer subtypes. *Proc. Natl. Acad. Sci. U. S. A.* **107**, 15449-54.

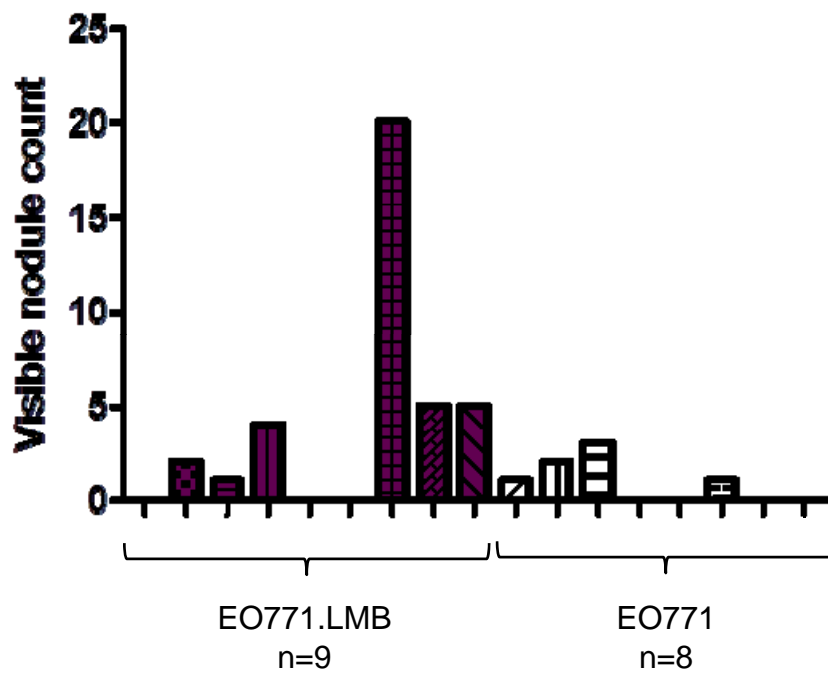
A



B

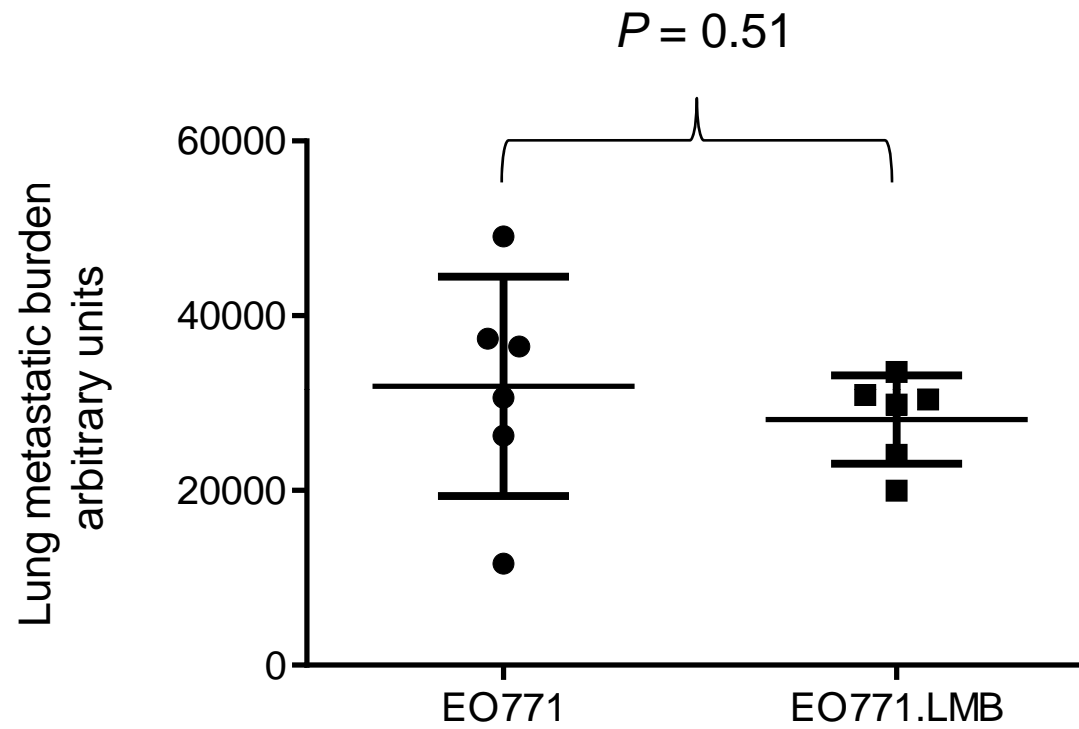
| Tumour | Overall Grade | Tubule Formation Score | Nuclear Pleomorphism Score | Mitosis Score | Mitoses per 10 HPF |
|--------------------|---------------|------------------------|----------------------------|---------------|--------------------|
| 67NR-A | 3 | 3 | 2 | 3 | 29 |
| 67NR-B | 3 | 3 | 2 | 3 | 32 |
| 4T1.2-A | 3 | 3 | 3 | 2 | 15 |
| 4T1.2-B | 3 | 3 | 3 | 3 | 42 |
| EO771-A | 3 | 3 | 3 | 3 | 27 |
| EO771-B | 3 | 3 | 3 | 3 | 90 |
| EO771.LMB-A | 3 | 3 | 3 | 3 | 57 |
| EO771.LMB-B | 3 | 3 | 3 | 3 | 66 |

Supp. Figure 1

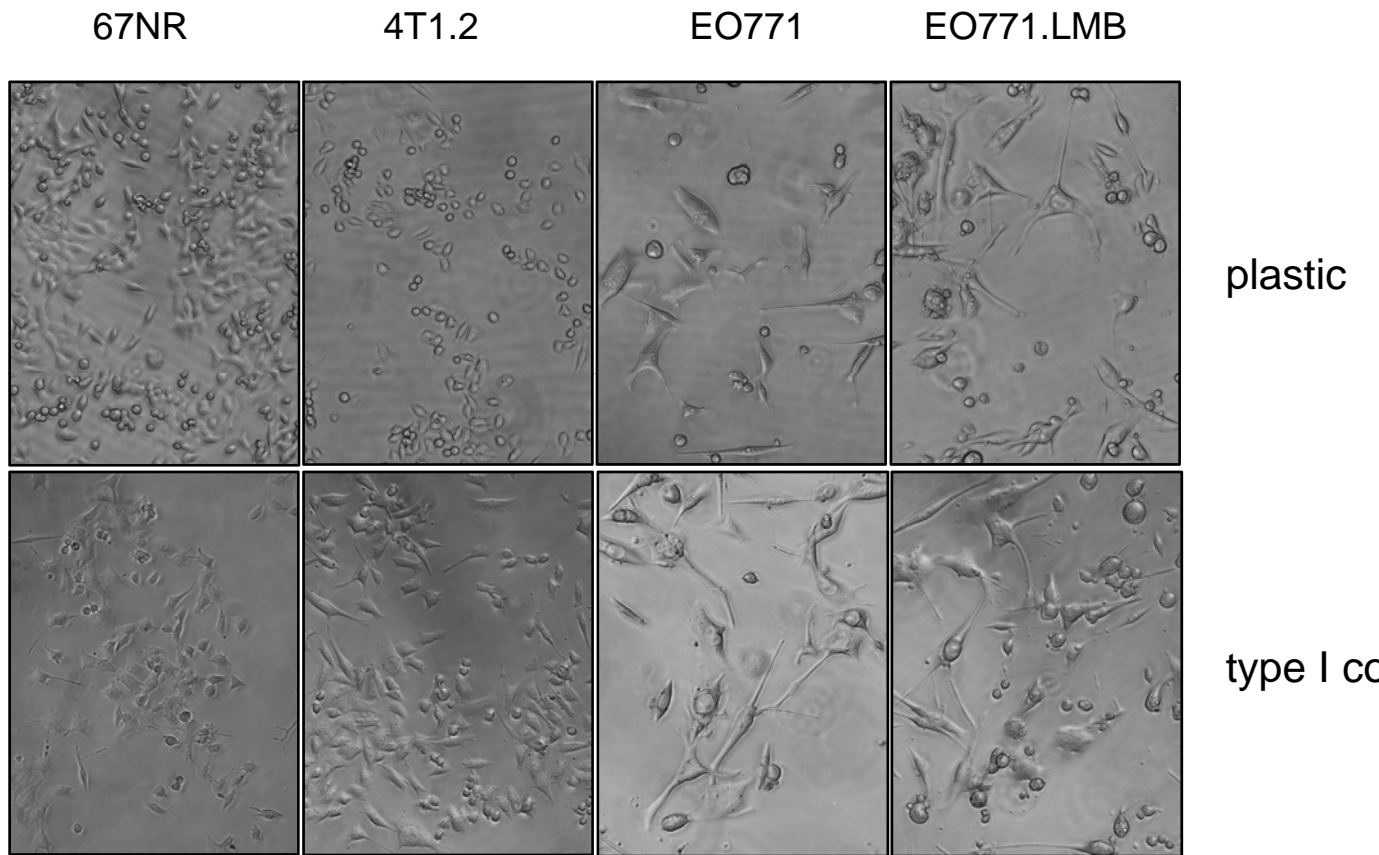


$$P = 0.20$$

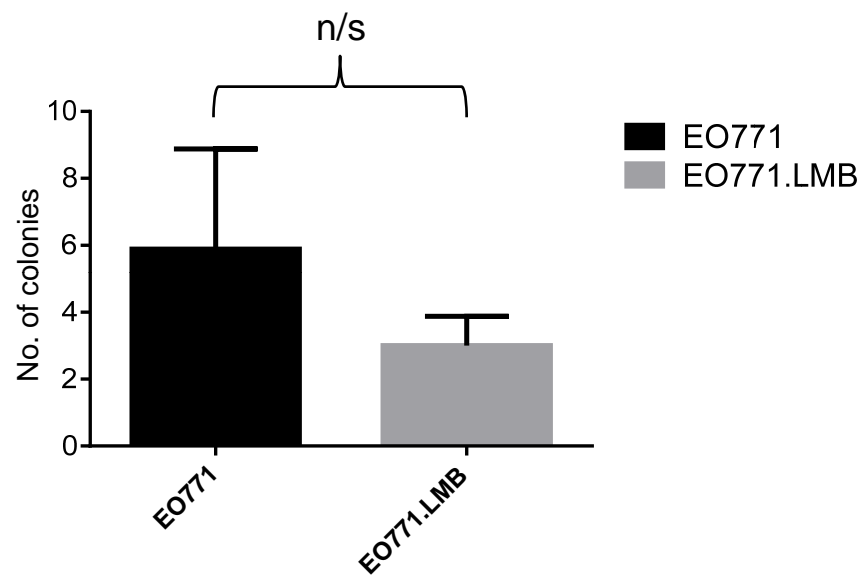
Supp. Fig. 2



Supp. Figure 3

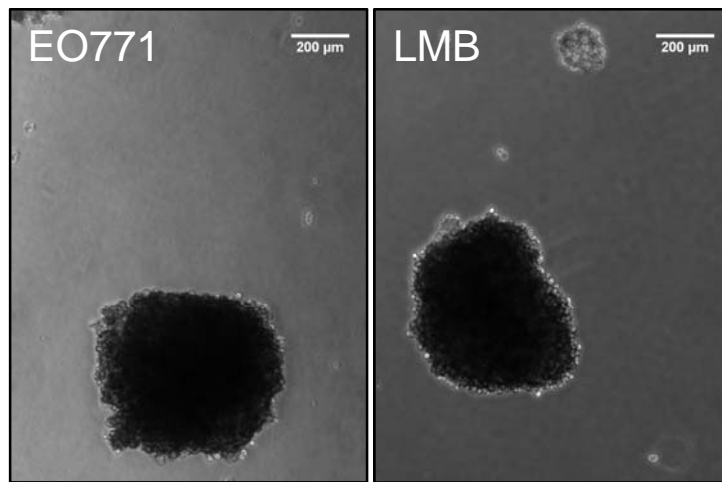


Supp. Figure 4

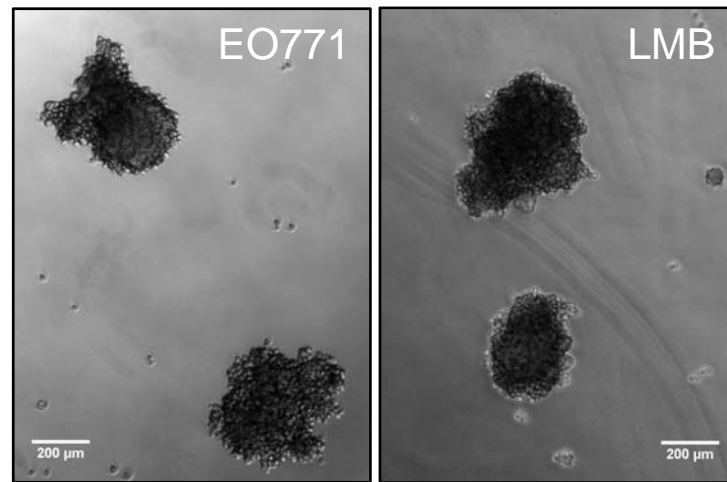


Supp. Figure 5

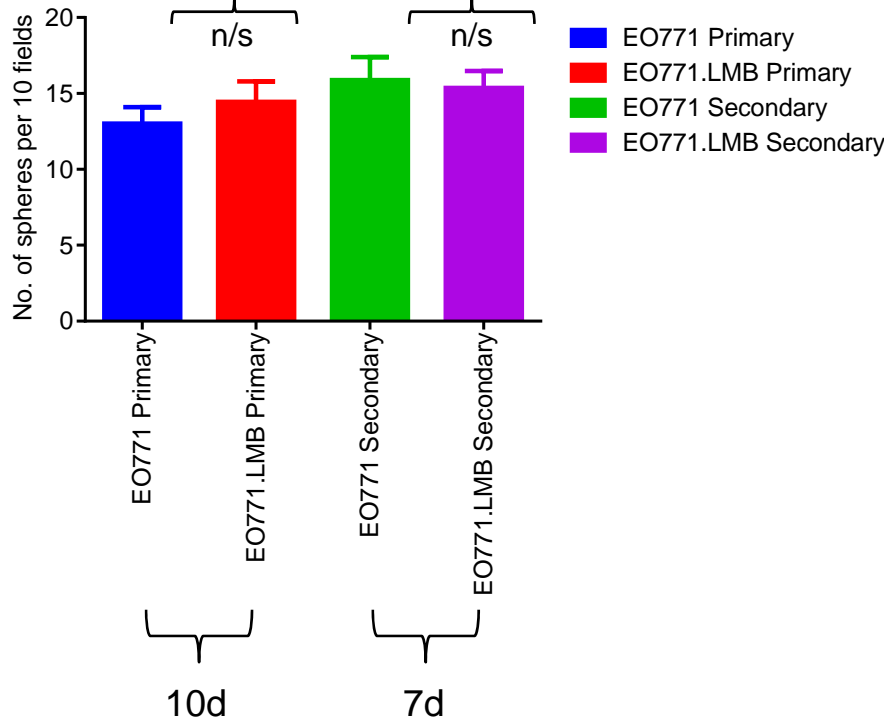
A



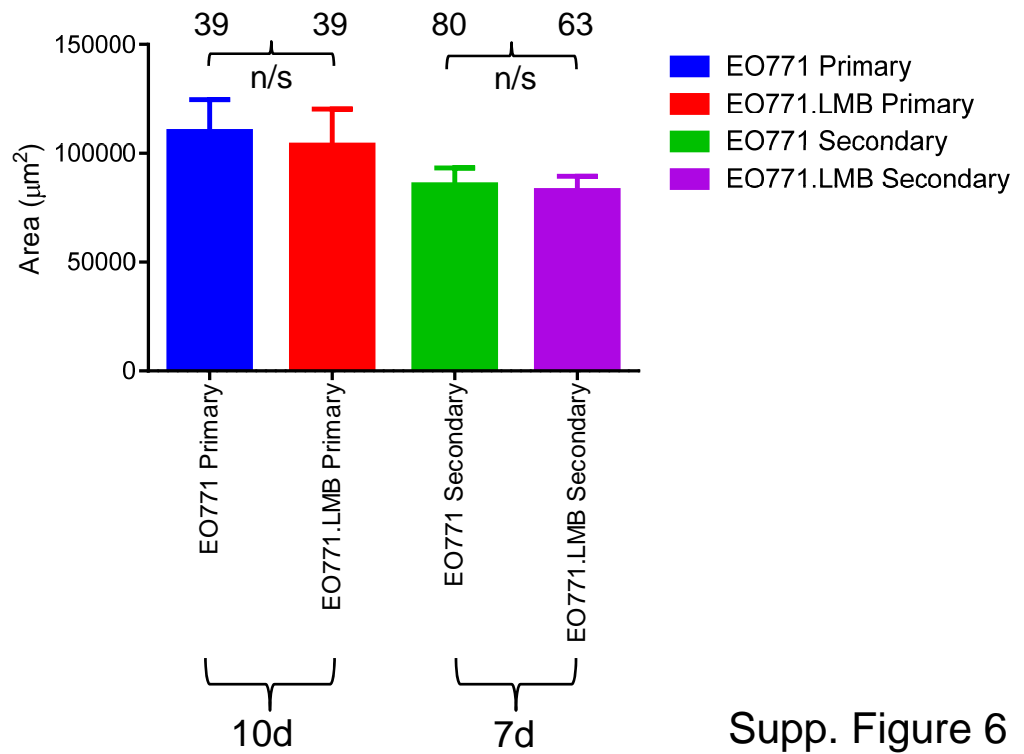
B



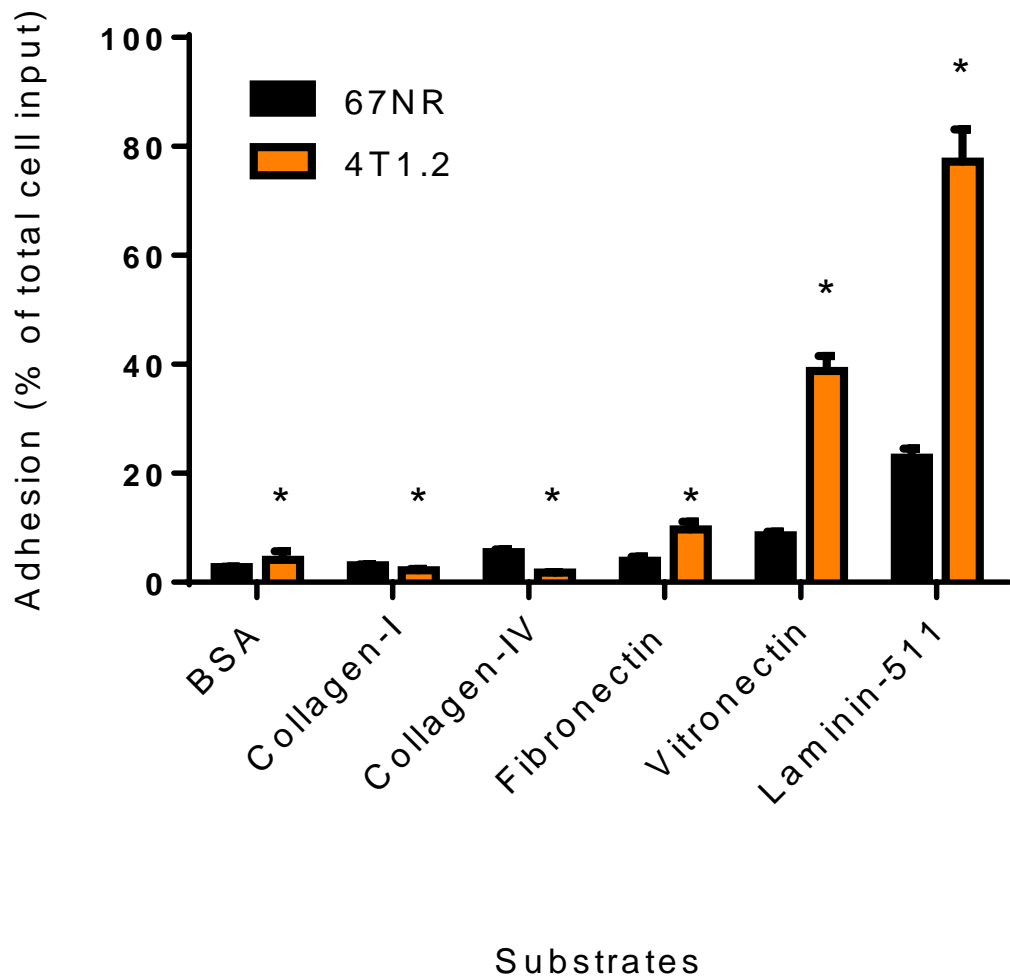
C



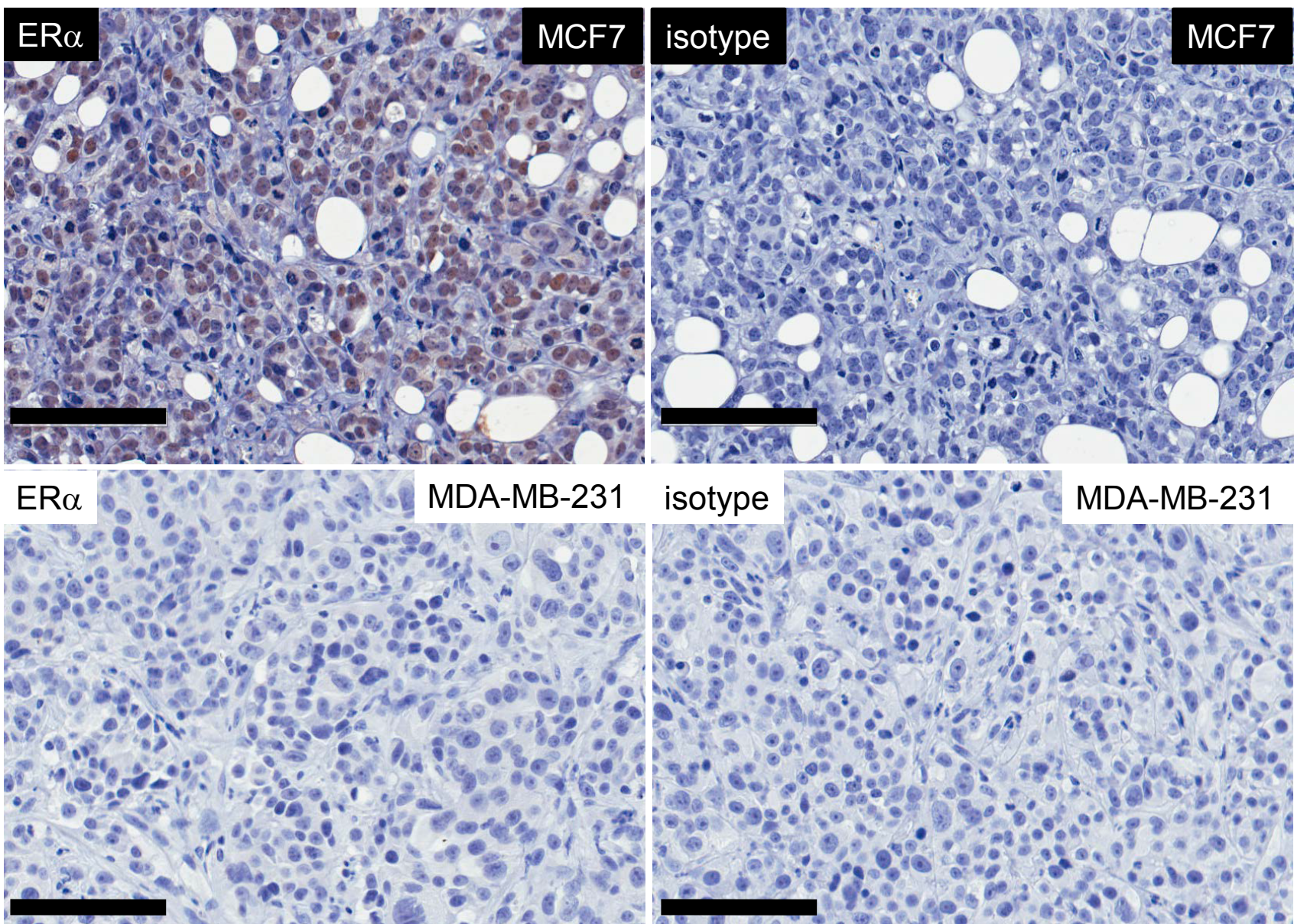
D



Supp. Figure 6

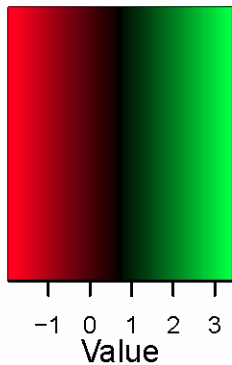


Supp. Figure. 7

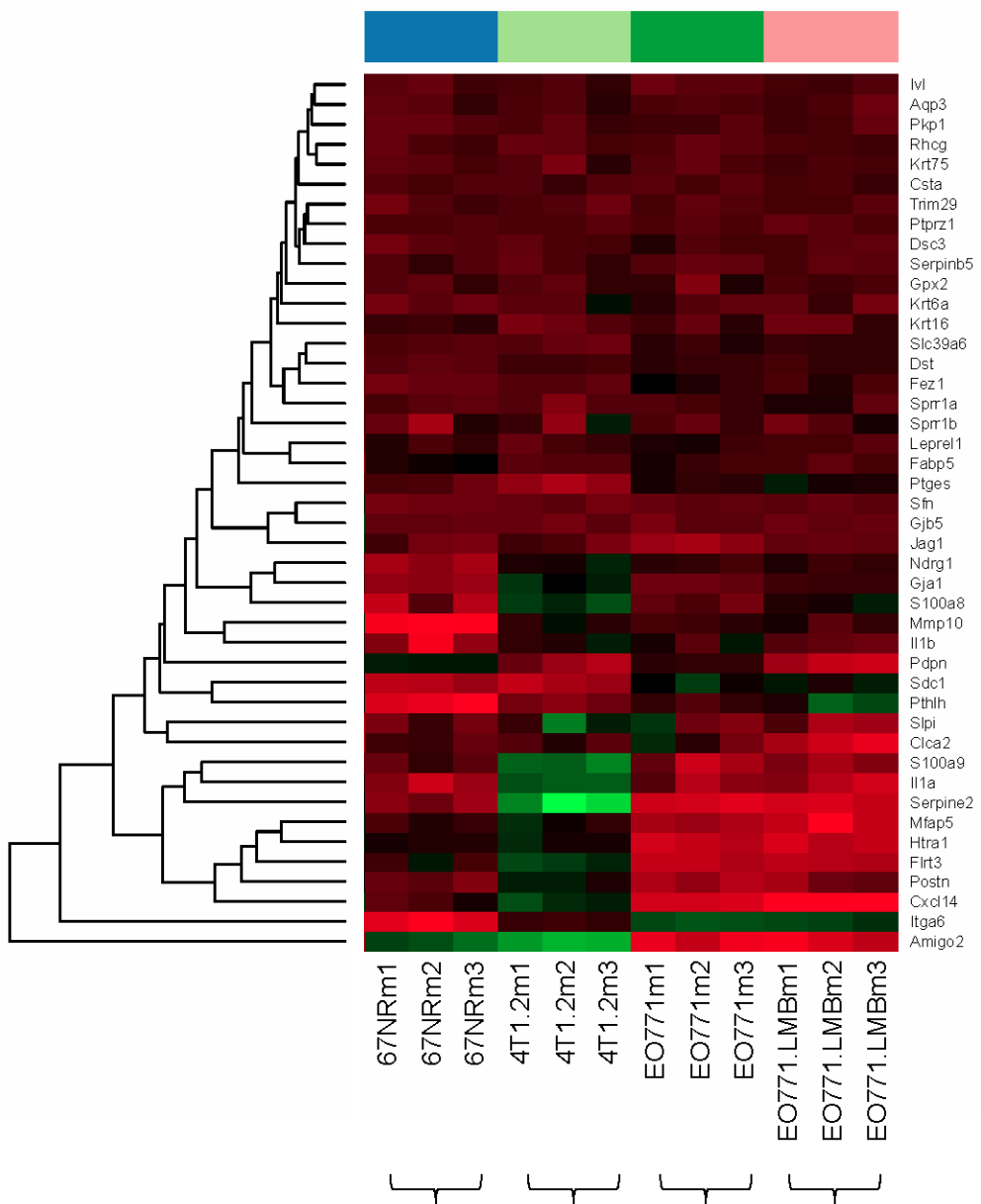


Supplementary Figure 8

Color Key

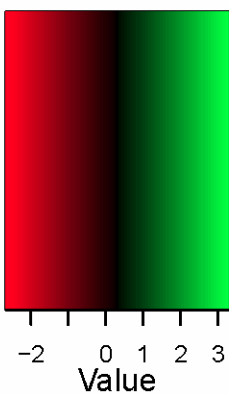


BASAL

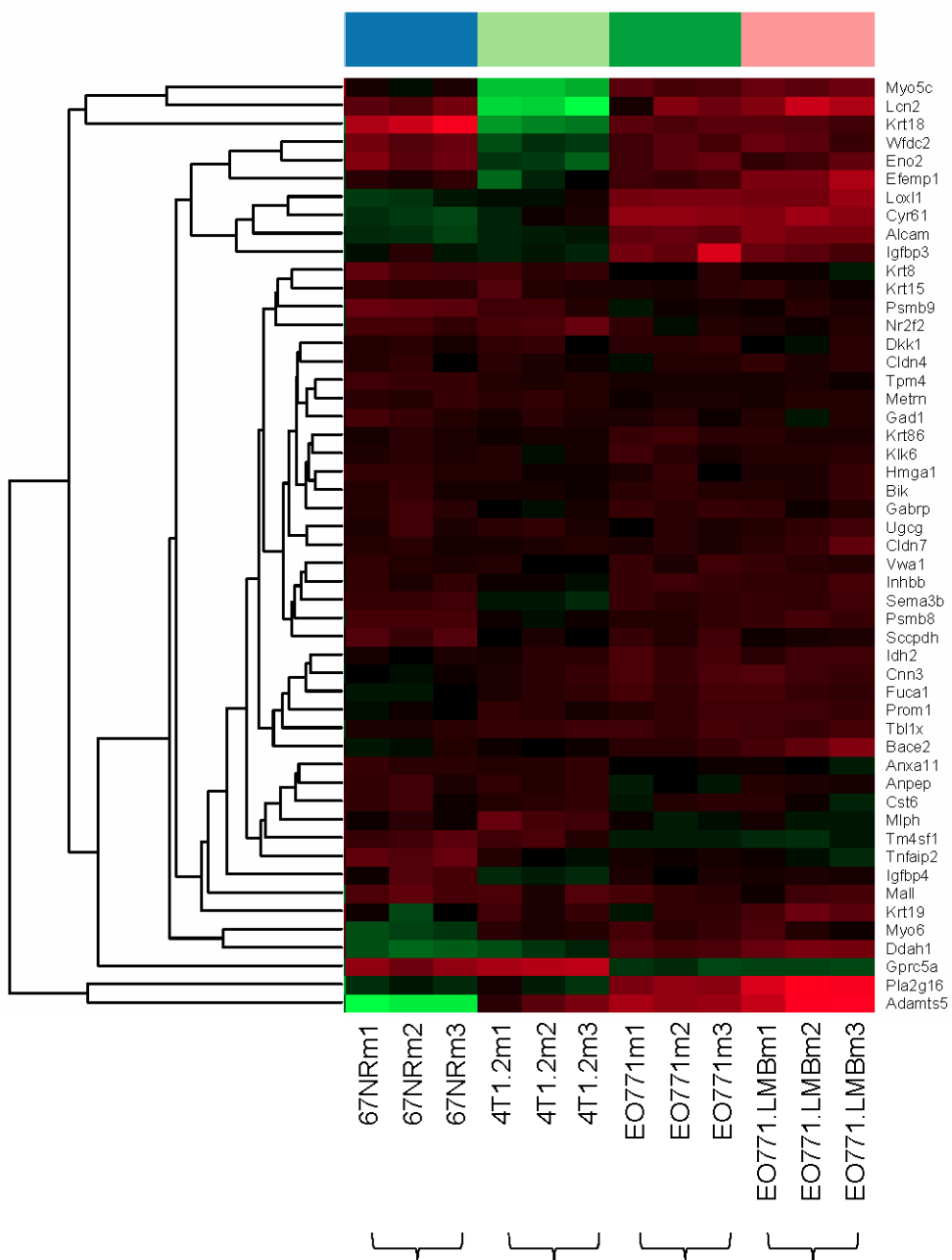


Supp. Figure 9A

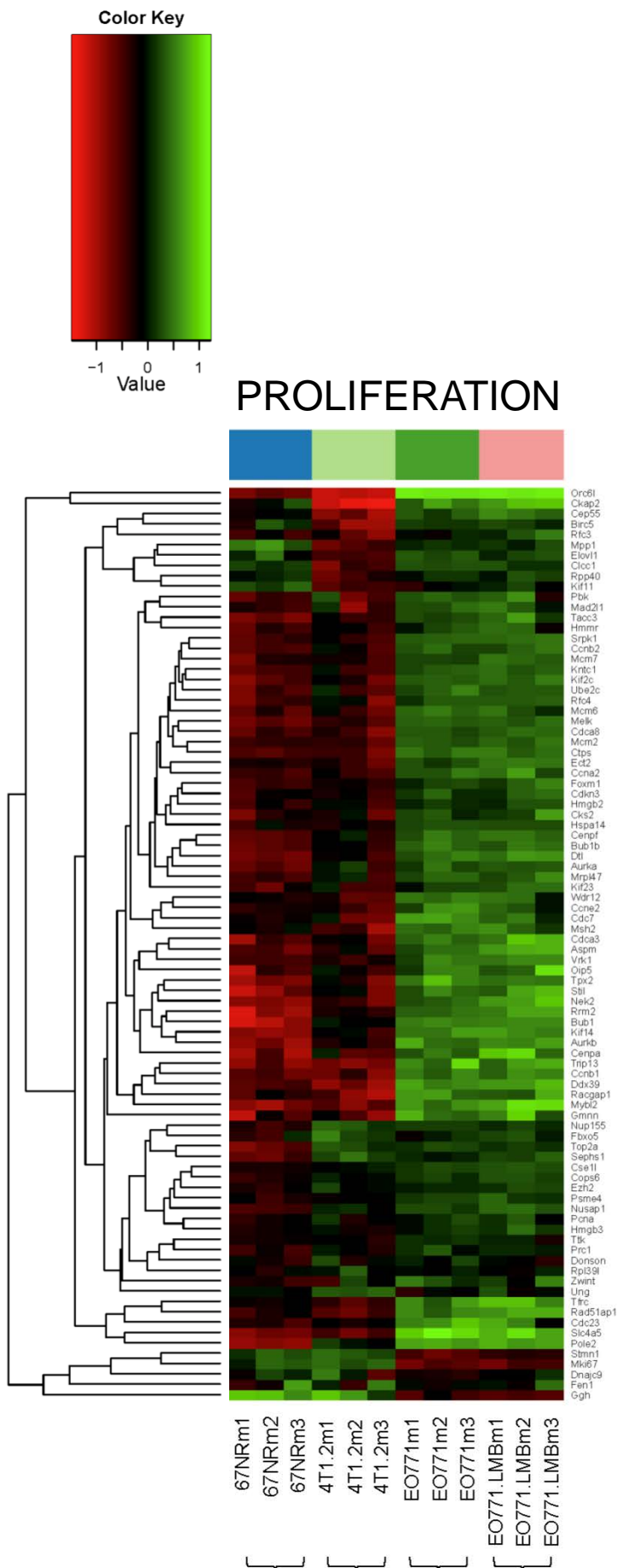
Color Key



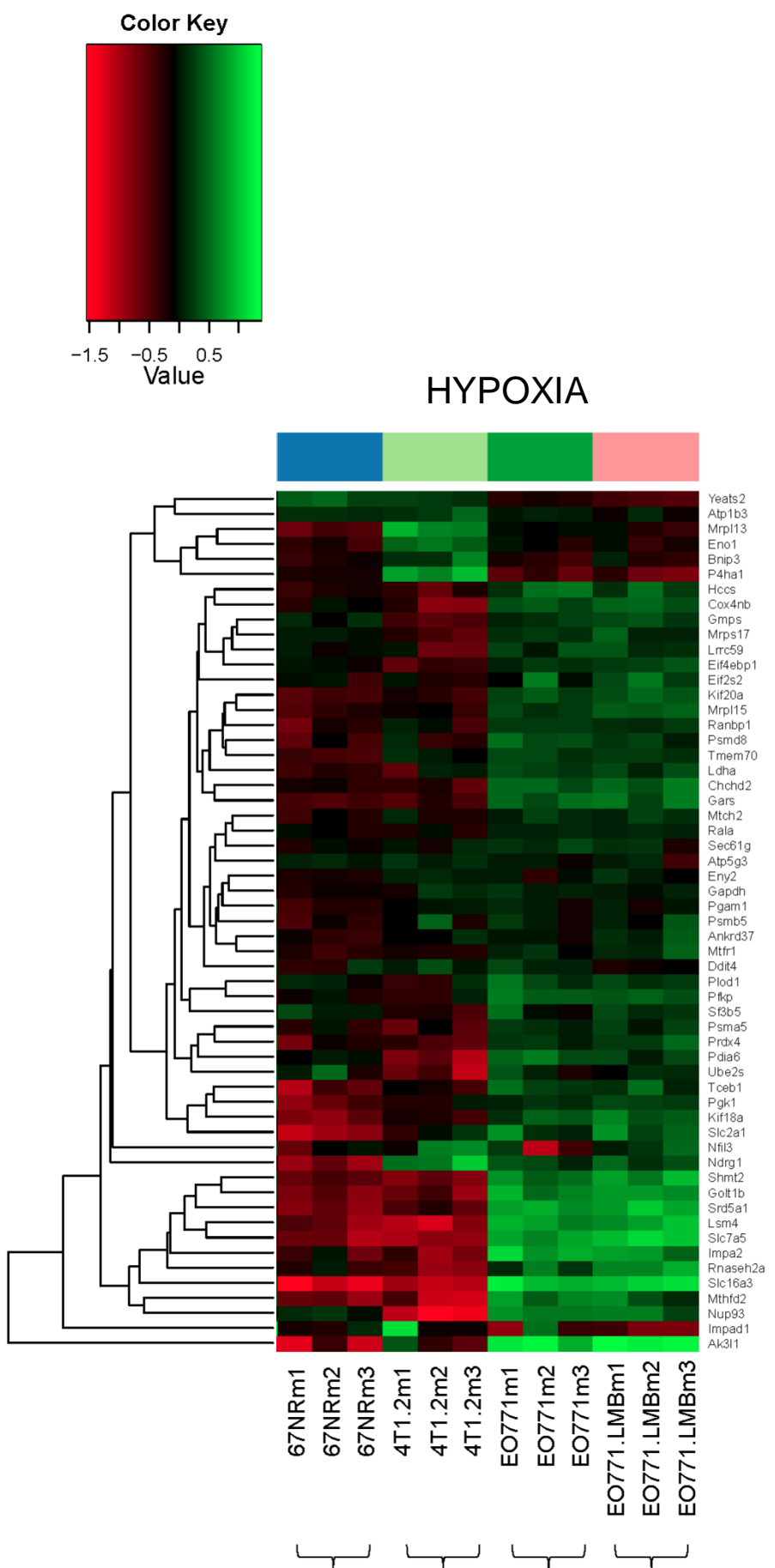
LUMINAL



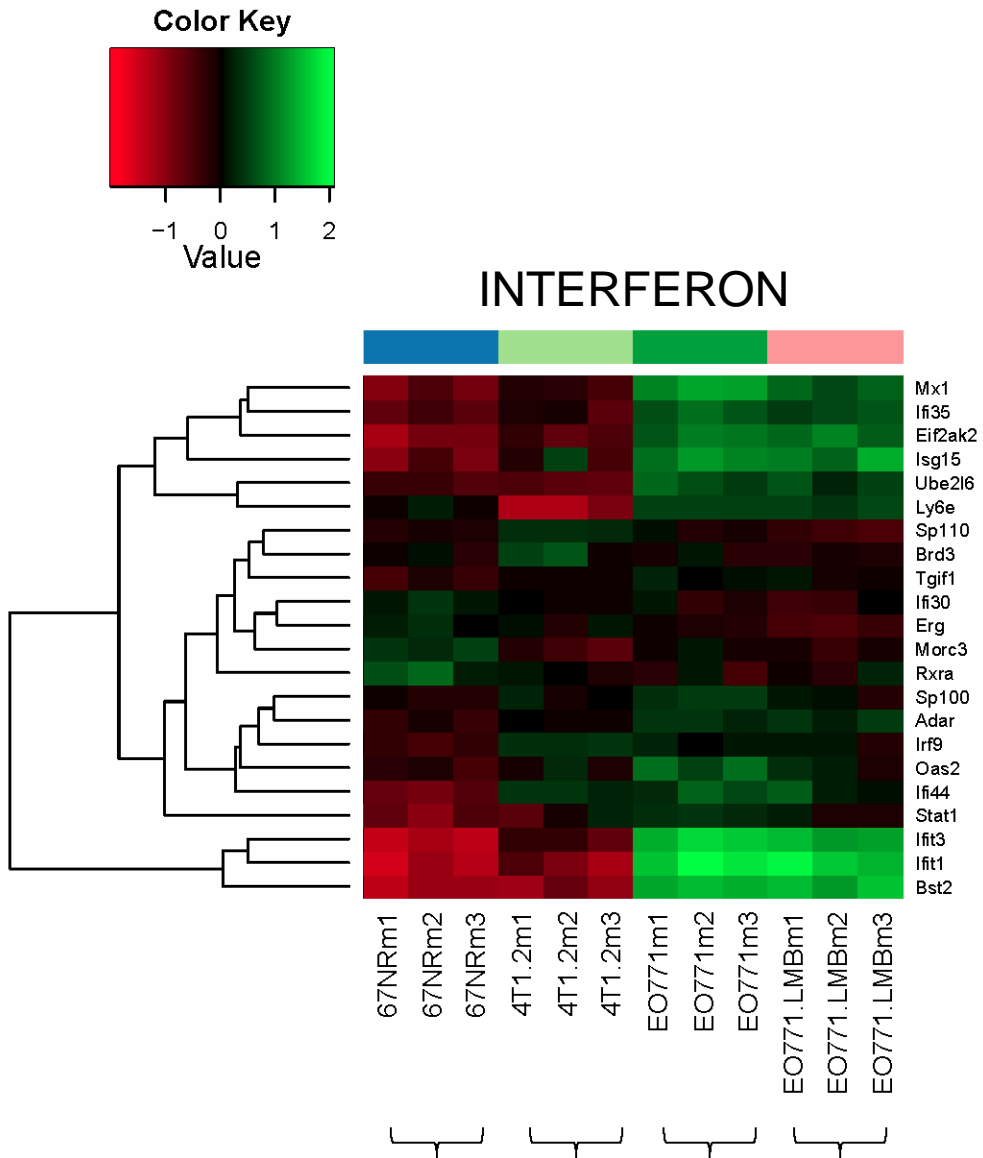
Supp. Figure 9B



Supp. Figure 9C

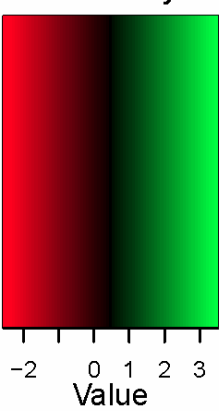


Supp. Figure 9D

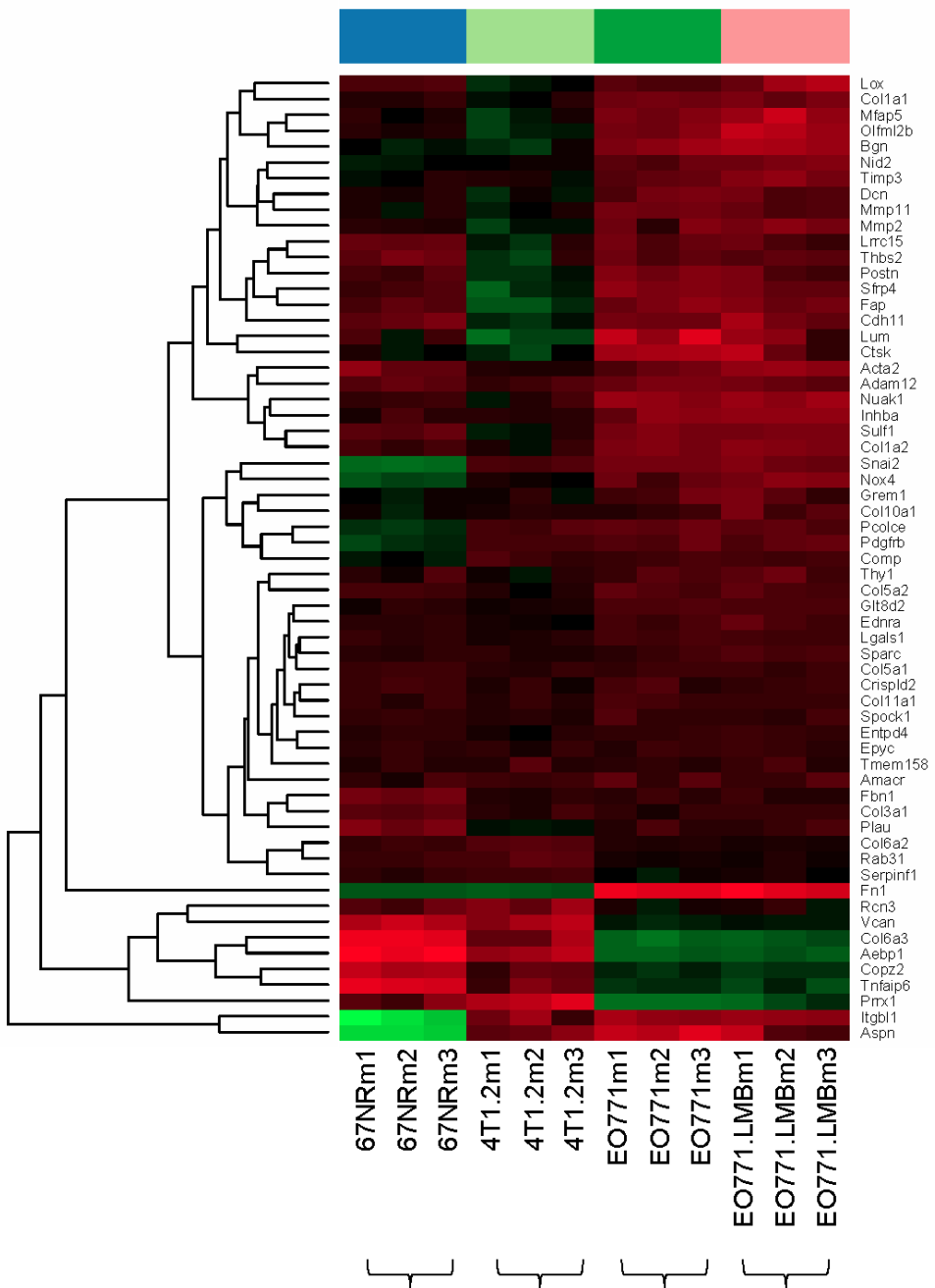


Supp. Figure 9E

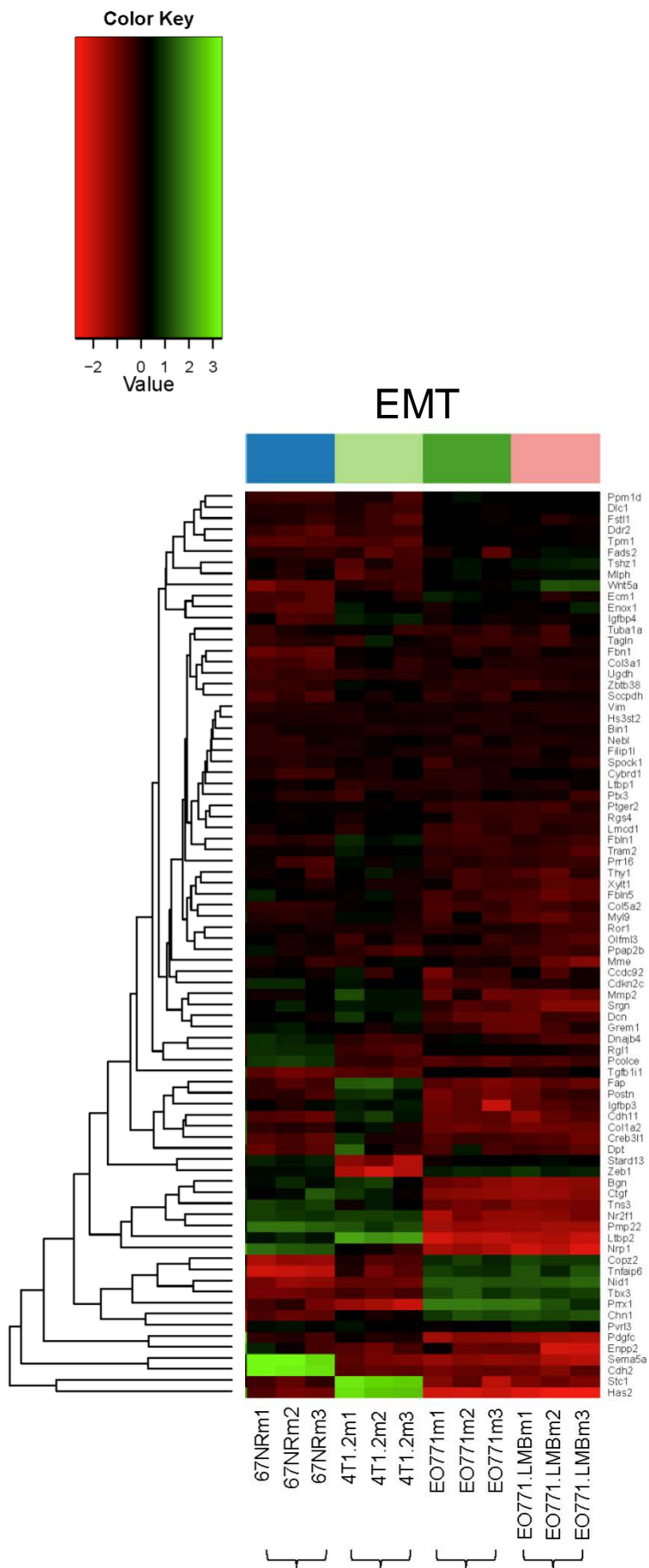
Color Key



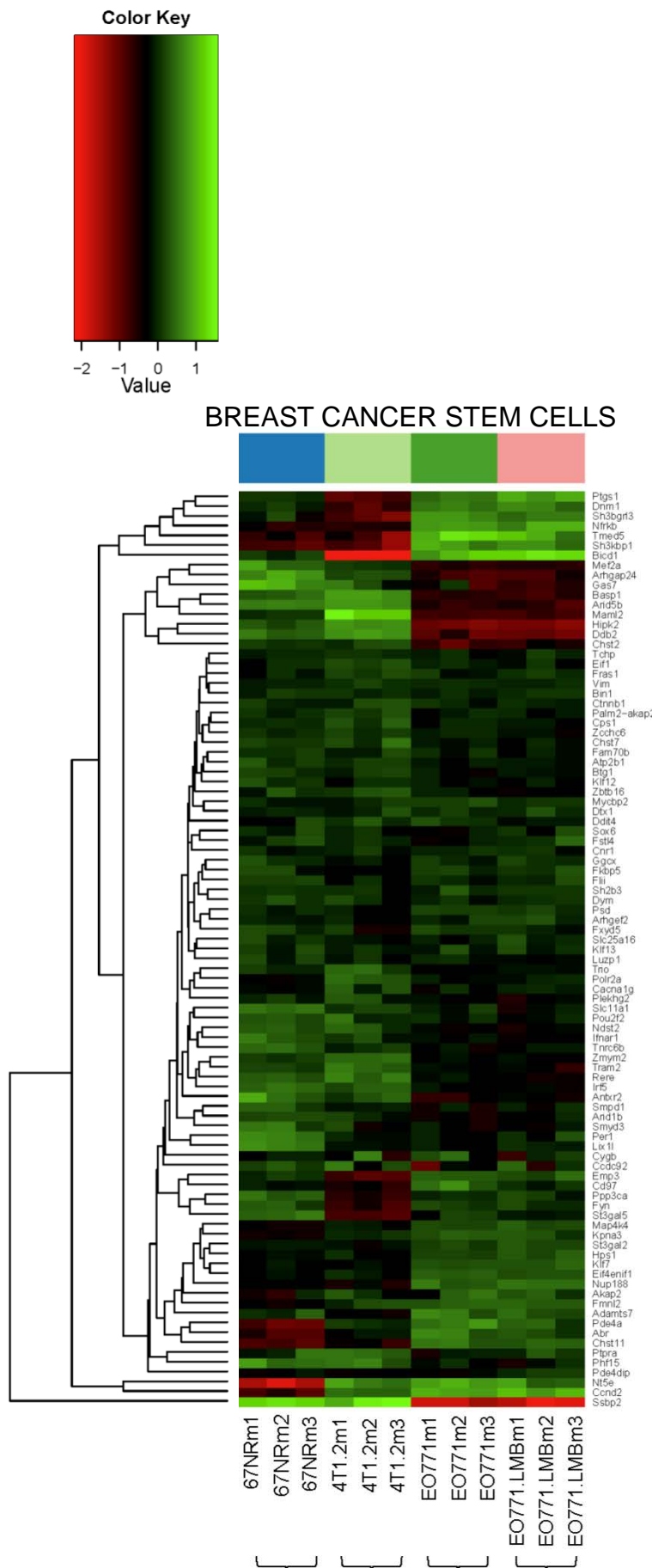
INVASION



Supp. Figure 9F



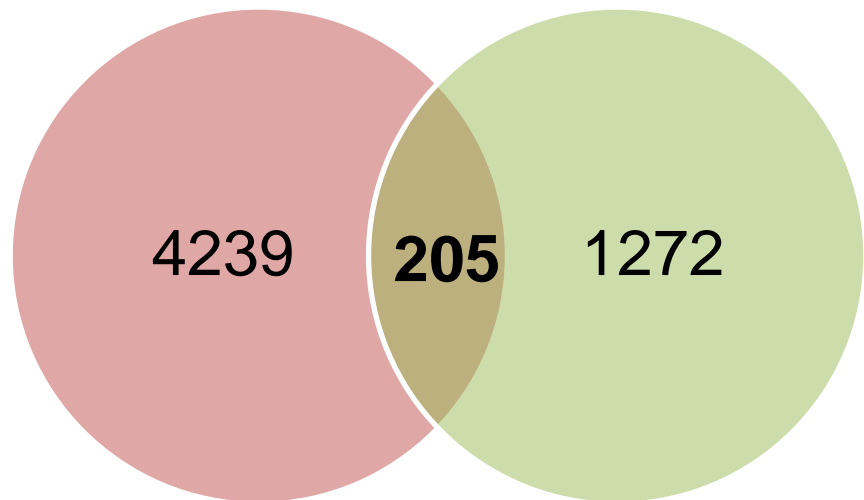
Supp. Figure 9G



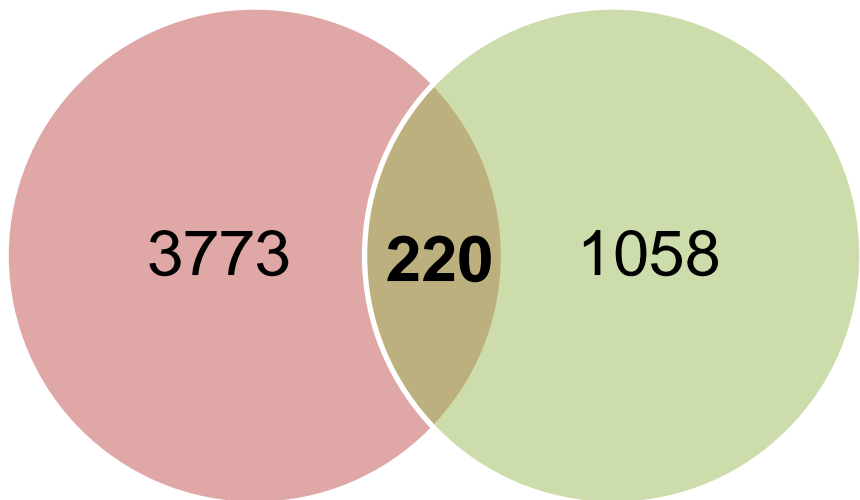
Supp. Figure 9H

Supplementary Figure 10

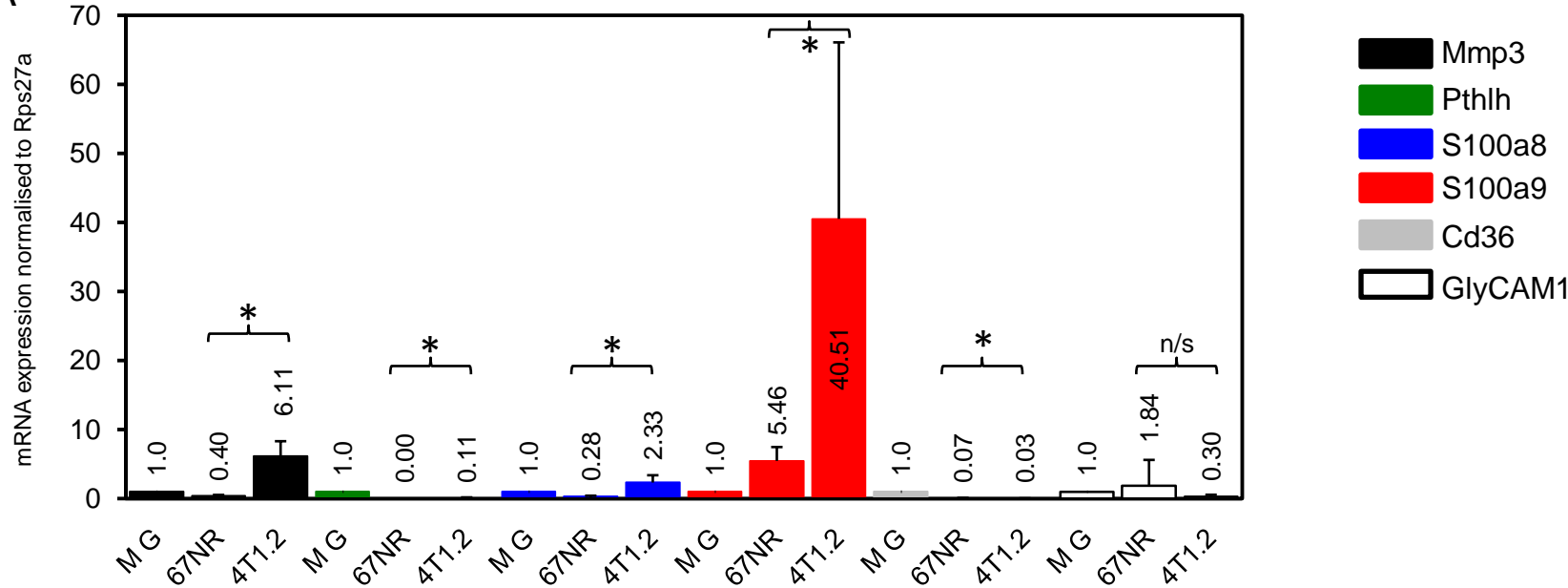
A. Upregulated



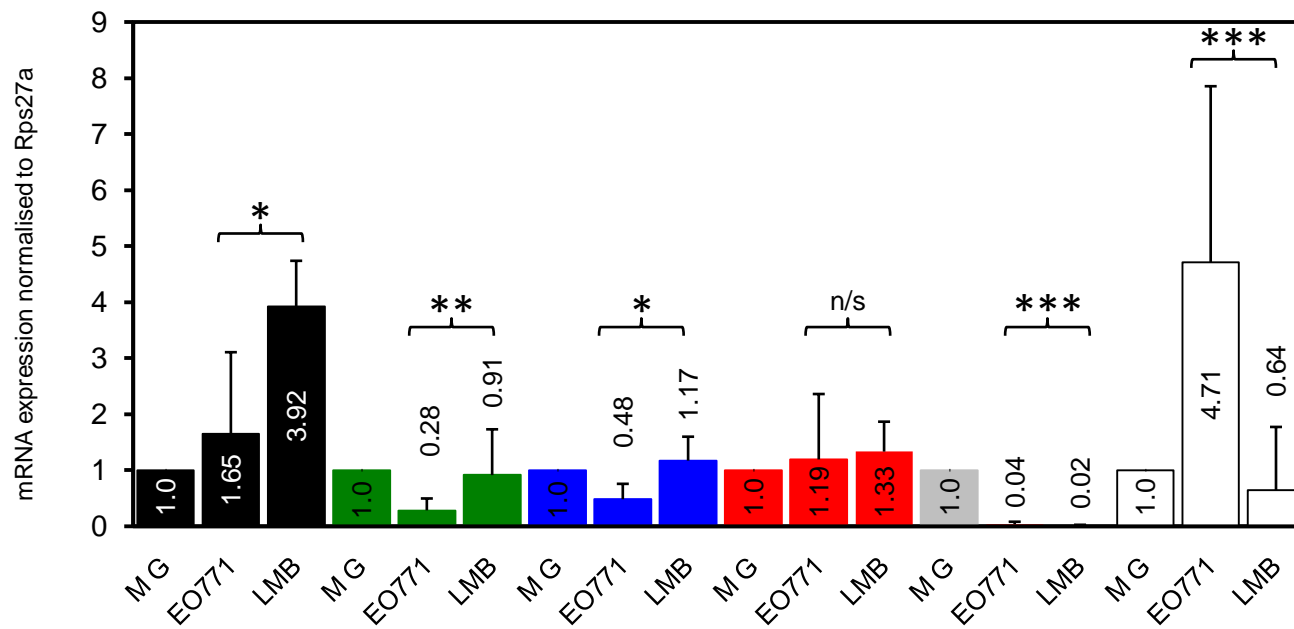
B. Downregulated



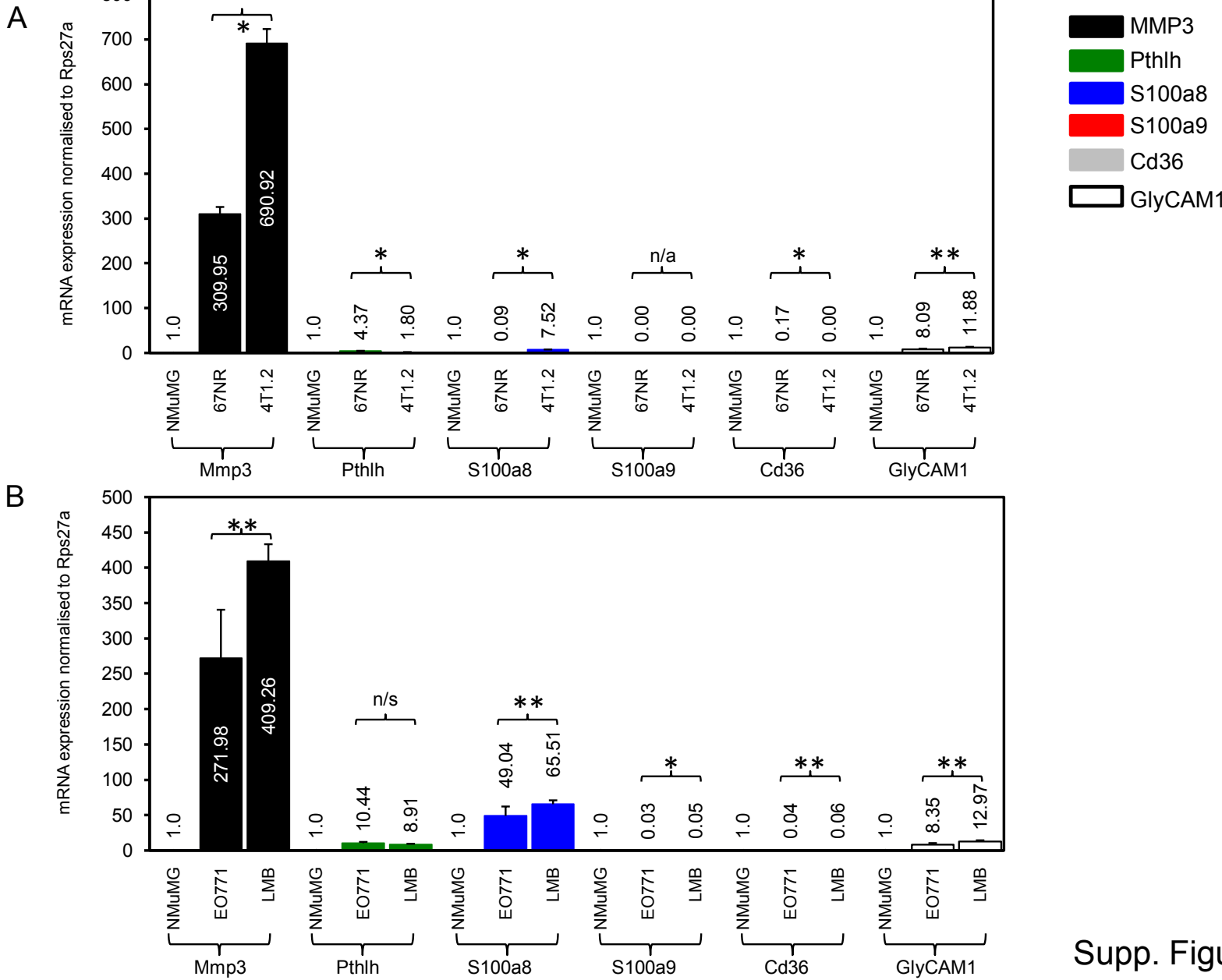
A



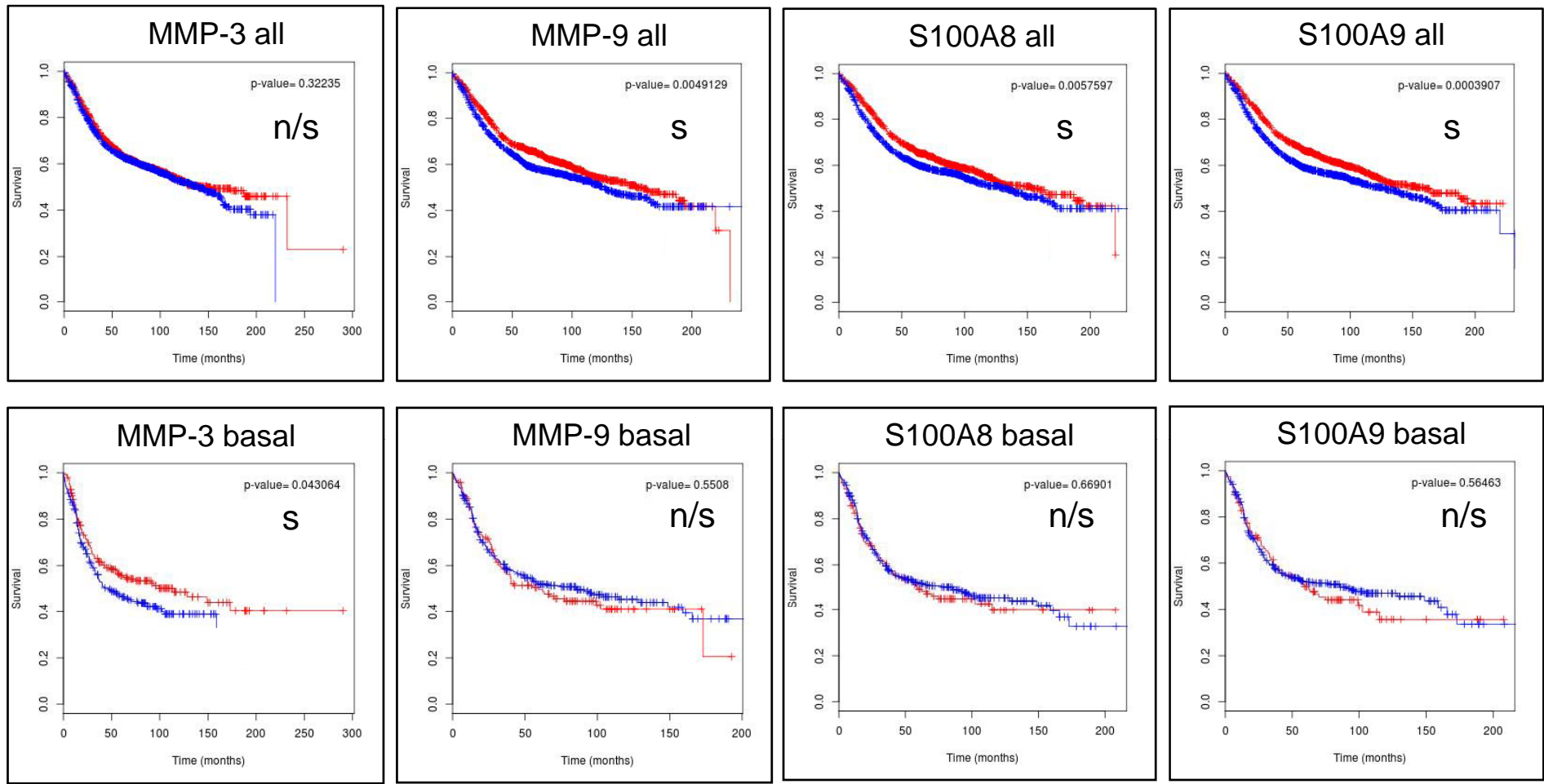
B



Supp. Figure 11



Supp. Figure 12



Supplementary Figure 13

Supplementary Table 1

| Signature | 67NR | 4T1.2 | EO771 | EO771.LMB |
|---|----------|-----------------|---|---|
| BASAL sig-UP | 4 (9%) | 11 (23%) | 5 (11%) | 5 (11%) |
| | 11 (23%) | 3 (6%) | 11 (23%) | 10 (21%) |
| | 32 (68%) | 33 (70%) | 31 (66%) | 32 (68%) |
| LUMINAL sig-UP | 10 (18%) | 15 (27%) | 4 (7%) | 8 (15%) |
| | 14 (25%) | 3 (5%) | 17 (31%) | 15 (27%) |
| | 31 (56%) | 37 (67%) | 34 (62%) | 32 (58%) |
| PROLIFERATION sig-UP | 6 (6%) | 4 (4%) | 50 (48%) | 57 (54%) |
| | 61 (58%) | 24 (23%) | 5 (5%) | 4 (4%) |
| | 38 (36%) | 77 (73%) | 50 (48%) | 44 (42%) |
| HYPOXIA sig-UP | 3 (3%) | 6 (5%) | 28 (25%) | 29 (25%) |
| | 43 (38%) | 17 (15%) | 5 (4%) | 2 (2%) |
| | 68 (60%) | 91 (80%) | 81 (71%) | 83 (73%) |
| EMT sig-UP | 22 (24%) | 16 (17%) | 16 (17%) | 15 (17%) |
| | 27 (29%) | 13 (14%) | 29 (31%) | 28 (30%) |
| | 44 (47%) | 64 (69%) | 48 (52%) | 50 (54%) |
| INTERFERON sig-UP | 1 (4%) | 3 (12%) | 9 (35%) | 13 (50%) |
| | 13 (50%) | 3 (12%) | 3 (12%) | 1 (4%) |
| | 12 (46%) | 20 (77%) | 14 (54%) | 12 (46%) |
| CANCER STEM CELLS sig-UP | 23 (23%) | 20 (20%) | 17 (17%) | 20 (20%) |
| | 15 (15%) | 17 (17%) | 18 (18%) | 18 (18%) |
| | 62 (62%) | 63 (63%) | 65 (65%) | 62 (62%) |
| INVASION sig-UP | 13 (20%) | 14 (22%) | 8 (13%) | 9 (14%) |
| | 17 (27%) | 10 (16%) | 30 (47%) | 31 (48%) |
| | 34 (53%) | 40 (63%) | 26 (41%) | 24 (38%) |
| SIGNIFICANT GENE EXPRESSION SIGNATURES | | LUMINAL | PROLIFERATION HYPOXIA INTERFERON | PROLIFERATION HYPOXIA INTERFERON |

Supplementary Table 4: Sequences of oligonucleotide primers used for qRT-PCR

| Gene | Forward Sequence | Reverse Sequence |
|--------|----------------------------------|--------------------------------|
| Pthrp | 5' TTC GGT GGA GGG GCT TGG CC | 5' CGG CGG CGC AAG TCT TGG AT |
| S100a8 | 5' CAC CAT GCC CTC TAC AAG AAT G | 5' TCA CCA TCG CAA GGA ACT CC |
| S100a9 | 5' GGA AGC ACA GTT GGC AAC | 5' TCC AGG TCC TCC ATG ATG TCA |
| Egfr | 5' CTG TCG CAA AGT TTG TAA TG | 5' GAA TTT CTA GTT CTC GTG GG |
| MMP-9 | 5' CCA GAC ACT AAA GGC CAT TCG A | 5' TCC CAC TTG AGG CCT TTG AAG |
| Rps27a | 5' GAC CCT TAC GGG GAA AAC CAT | 5' AGA CAA AGT CCG GCC ATC TTC |